UC San Diego

UC San Diego Electronic Theses and Dissertations

Title

Using Deep Two-Photon Microscopy to Test the Dentate Gate Hypothesis

Permalink

https://escholarship.org/uc/item/43t4225b

Author

Tran, Thanh

Publication Date

2017

Peer reviewed|Thesis/dissertation

eScholarship.org Powered by the California Digital Library
University of California

UNIVERSITY OF CALIFORNIA, SAN DIEGO

Using Deep Two-Photon Microscopy to Test the Dentate Gate Hypothesis

A Thesis submitted in partial satisfaction of the requirements for the degree Master of Science

in

Biology

by

Thanh Duy Tran

Committee in Charge:

Professor Fred Gage, Chair
Professor Nigel Crawford, Co-Chair
Professor Randolph Hampton

2017

The Thesis of Thanh Duy Tran is approved, and it is acceptable in quality and form for publication on microfilm and electronically:

Co-Chair

Chair

University of California, San Diego

2017

TABLE OF CONTENTS

LIST OF FIGURES

List of Tables

ACKNOWLEDGEMENTS

I would like to thank Dr. Fred Gage, Dr. Nigel Crawford, and Dr. Randolph Hampton for agreeing to be on my committee and supporting my research efforts. I would also like to acknowledge Dr. Matthew Shtrahman, Cooper Bloyd, Shannon Kee, Alexander Newberry, Nolan Mac, Sarah Parylak, Stacy Kim, and Ondrej Novak for their contributions to this project.

ABSTRACT OF THE THESIS

Using Deep Two-Photon Microscopy to Test the Dentate Gate Hypothesis

by

Thanh Duy Tran

Master of Science in Biology

University of California, San Diego, 2017

Professor Fred Gage, Chair

Professor Nigel Crawford, Co-Chair

Mesial temporal lobe epilepsy is the most common form of epilepsy in adults, but the underlying mechanisms are still not yet understood. Pathological changes in mTLE are prominent in the dentate gyrus (DG), a region important for regulating

activity in the hippocampus and one of only two regions in the mammalian brain where adult neurogenesis occurs. Both human and animal studies of mTLE demonstrate defects in the migration and function of immature adult-born dentate granule cells. In this study, we gained further insight into mTLE using the pilocarpine murine model. Using a new generation of red calcium sensors and long wavelength two-photon excitation, we were able to image network activity within the intact hippocampus of awake behaving mice. This study took advantage of a surgical approach to implant a cranial imaging window on top of the hippocampus. Populations of labeled cells were chronically imaged in vivo. The DG in epileptic mice demonstrated synchronous firing, as seen by numerous flashes in the videos where multiple cells fired at the same time, which was not observed in the control mice. In vivo calcium imaging of the deeper brain tissue allows us to understand more about the dynamics of the layers, but this technique has its limitations. There were difficulties in obtaining a large enough sample size of mice as many cohorts of mice did not have the jRGECO protein expression in the DG. This study has set the groundwork for future experiments elucidating the role of immature adult-born DGCs in epileptogenesis.

Chapter 1. Introduction

Mesial temporal lobe epilepsy (mTLE) is the most common form of epilepsy in adults. The most common pathology associated with mTLE is hippocampal sclerosis (Engel et al 2001). Symptoms associated with temporal lobe epilepsy are disabling seizures, deficits in attention, memory, executive functions, mood, and personality. These symptoms arise from the activation or inhibition of areas in the temporal lobe, which involve a wide range of functions such as auditory, olfactory, visual, memory, emotional, and social functions. The temporal lobe contains both the phylogenetically older medial temporal cortex which includes the olfactory areas, amygdala, hippocampus and parahippocampal gyrus and the lateral (neocortical) temporal cortices which are divided into anterior, superior, and inferior regions (Devinsky 2004). Approximately 40% of patients with mTLE are resistant to antiepileptic drugs, with the most effective treatment for medically refractory mTLE being temporal lobe resection. The success rate of temporal lobe resection in reducing seizures in this population has ranged from 70% to 90%. However, not all patients are eligible for temporal lobe surgery. Patients with extrahippocampal pathology or bilateral disease are not considered optimal candidates because of the higher possibility of seizure recurrence (Vale et al 2012).

The hippocampus is considered to have an important role in epileptogenesis as it undergoes morphological changes and network reconstruction upon seizure induced damage. The hippocampus in mTLE has many abnormalities such as CA1 and CA3 pyramidal cell loss, hippocampal astrogliosis, and damage to the hilus of the DG. Key

pathological features also found are mossy fiber sprouting, granule cell layer dispersion, ectopically-located dentate granule cells (DGCs), and DGCs with prominent hilar basal dendrites (Parent et al 2012). Hippocampal sclerosis is the most common pathology observed in mTLE patients, and unilateral excision of the hippocampus has been observed to reduce seizure incidence in mTLE patients (Engel et. al 2001). The dentate gyrus (DG), hippocampus proper (consisting of CA1-CA4 sub-regions), and the subiculum compose the hippocampal formation, which has an important role in learning and memory. Sensory information is guided by sensory cortices, funneled by the EC, and then sent through the DG to CA3 to CA1, completing a loop called the tri-synaptic circuit. Layer two of the EC sends the main sensory inputs to the DG. The neurons from the EC project axons along the perforant pathway, which synapse onto the dendritic spines of DG neurons within the molecular layer. The tri-synaptic circuit then continues as DG synapse onto pyramidal neurons within the CA3 sub-region of the hippocampus via mossy fibers as well as interneurons in the hilus (Toni et al., 2008). The pyramidal neurons of CA3 next project axons along the Shaffer collateral pathway onto pyramidal neurons within the CA1 sub-region of the hippocampus. These cells project back to layer 4/5 of the entorhinal cortex to cortical association regions, completing the tri-synaptic circuit and allowing us to process our sensory information. However, the term “trisynaptic circuit” does not represent the entire flow of information. For example, the EC has a more direct pathway to CA3, bypassing the DG. The EC also makes a direct connection to CA1 via the temporammonic pathway (Scharfman, 2007).

Despite the constant inputs from the EC to the DG, the DG demonstrates sparse activity (Piatti et al 2013). This sparse activity in the DG plays an important role in memory formation and recall, and regulates the activity throughout the rest of the hippocampus. The DG is thought to be important for pattern separation, where similar input firing patterns from the EC can result in similar but distinct output firing patterns in the DGCs. Pattern separation has been suggested to be important for coding similar, yet distinct, behavioral experiences into different memories (Deng et. al 2010). The DG is thought to have a pattern separation function because of several key characteristics of the DG. Neuroanatomical studies have illustrated that the DG has about ten times more cells than the EC (Amaral 2007). The inputs from the EC are expanded onto the increased number of DGCs (McNaughton and Morris 1987).

Despite the large number of DGCs, only 1-2% of the total cells are active in a given behavioral experience as shown by labeling cells that express immediate early genes such as c-Fos (Chawla et. al 2005). One mechanism that may contribute to the sparse firing of the DGCs is that these cells have a hyperpolarized resting membrane potential of -84mV, needing higher inputs to reach threshold (Staley et. al 1992).

Another important contribution to the sparse firing of this network is the strong feedforward and feedback inhibition that the DGCs receive from neighboring cells. Hilar inhibitory interneurons are located deep to the granule cell layer and are synapsed by axons projecting from the EC, DGCs, and hilar mossy cells (Piatti et al 2013). These inhibitory neurons have high intrinsic firing rates and are important for inhibiting DGCs. This inhibition is thought to contribute to the sparse activity in the

DG and regulate the spreading of neuronal activity. In humans and animal models of mTLE, significant loss of somatostatin (SOM) expressing hilar interneurons has been observed (Houser et al 2014). Also seizure frequency in mice with pilocarpine induced epilepsy has been reduced by transplantation of inhibitory neural precursor cells into the hippocampus (Hunt et al 2013).

Adult neurogenesis is thought to be another important contribution to the sparse firing of the DG. The DG is one of two regions in the adult mammalian brain that continues to produce new neurons throughout adulthood. In the subgranular zone (SGZ) of the dentate gyrus of the hippocampus, there is a pool of the quiescent radial glia cells that occasionally divide to generate transiently amplifying neural progenitor cells (NPCs). After a few divisions, NPCs become immature neurons, which are post-mitotic and migrate into the DG granule cell layer where they differentiate into mature neurons. Mature granule cells in the DG have spines in the molecular layer of the hippocampus where they obtain input from the EC (O'Keefe and Nadel 1978). Their axons reach into the CA3 region of the hippocampal Ammon's horn and the hilus. They also innervate inhibitory interneurons in the hilus (Toni et al. 2008). The generation of new neurons in the DG of the hippocampus in adult mammals is thought to play a critical role in spatial learning and memory formation (Deng et al 2010). Aberrations in adult hippocampal neurogenesis have been implicated in epileptic seizures (Jessberger et al. 2007).

In contrast to mature DGCs, 4-6 week old adult-born DGCs have enhanced excitability and require less activation from presynaptic inputs to reach action

potential threshold (Piatti et al 2013) (Marin-Burgin et al 2015). Evidence suggests that these hyperexcitable immature DGCs actually contribute to the sparse activity in the DGCs (Piatti et al 2013), however the mechanism is unknown. Anatomical studies have shown that immature DGCs synapse onto hilar interneurons. In vivo electrophysiology studies in brain slices have found that these immature DGCs make weaker synapses than the mature DGCs (Temprana et al. 2015). However, the weaker synapses onto the hilar interneurons may be balanced by the enhanced excitability of immature DGCs.

In addition, the sparse firing of the DGCs is important for pattern separation function (Leutgeb et al. 2007) (deAlmedia et al. 2009). It may also have an important role in preventing seizure activity in epilepsy. Experiments suggest that the DG has an impaired ability to regulate and gate hippocampal activity (Heinneman et al 1992). Research into the dentate gate hypothesis has elucidated conflicting results. Labeling cells with c-Fos expression, the DG was the first region shown to become active in spontaneous seizures in pilocarpine treated animals (Peng and Houser 2005). Optogenetically silencing DGCs prevented seizure propagation in animal models of mTLE, providing in vivo evidence that DG activation is necessary for seizure propagation in mTLE (Krook-Magnuson et al 2015). In contrast, electrophysiology experiments have shown that CA1 pyramidal cells and not DGCs are hyperexcitable in response to synaptic inputs from the EC in rat models of mTLE (Ang et al 2006) (Coulter et al. 2011). Other studies suggest that the DG may be hyper-inhibited in mTLE (Sloviter et al. 2006).

One of the key pathological features observed in mTLE is mossy fiber sprouting, where axons from immature DGCs enter the molecular layer and activate other DGCs (Parent et. al 2012) (Sutula et. al 1989) (Babb et. al 1991). Mossy fibers are the axons of hippocampal DGCs that normally project to the pyramidal cells and interneurons of CA3 and to the hilus. This suggests a mechanism underlying the hyperexcitability. We hypothesize that in addition to direct excitation via mossy fiber sprouting, seizure activity inhibits the ability of immature DGCs to recruit hilar interneurons, resulting in hyperexcitability of mature DGCs (Fig. 1). In the study done by Hunt et. al, the decrease in seizures by the transplantation of inhibitory neural progenitors was not accompanied by a decrease in mossy fiber sprouting. This suggests that these aberrant synapses are not sufficient to cause seizures (Buckmaster et al. 2011). In this study, we aim to establish in-vivo 2 photon imaging as a tool to measure activity in distinct neuronal cell populations with single cell resolution, and perhaps definitively test the dentate gate hypothesis.

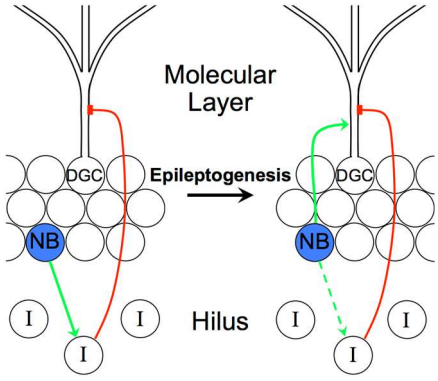

Figure 1. Hypothesized role of newborn DGCs in epileptogenesis. *Left:* In healthy animals Newborn (NB) DGCs recruit hilar interneurons (I), which inhibit mature DGCs and quiet the DG. *Right:* During epileptogenesis, NB DGCs lose their ability to drive hilar interneurons, & develop functional synapses onto mature DGCs, both contributing to DG hyperexcitability and seizures.

2-photon microscopy has significant benefits for neuroscience. Two-photon microscopy is an imaging technique that requires two photons, typically each with a wavelength in the near infrared range) to simultaneously excite a molecule, causing it to emit a photon with a wavelength within the visible range (Helmchen and Denk, 2006). The use of low energy, long wavelength photons (700-1000 nm) results in significantly less scattering of excitation light when imaging though deep tissue. The use of two photons in a small window of time to reach the energy threshold to excite a fluorophore reduces background signal and phototoxicity in imaging (Denk et al., 1990). These advantages have allowed for in vivo visualization of neural structures such as neurons, glial cells, and blood vessels. However, the single cell resolution of neuronal populations is typically limited to a maximal depth of ~500 μm. Since the DG lies ~ 1.7 mm below the surface of the cortex in mice, a conventional cortical cranial window would be unable to image the DG. To bypass this problem, the Gage lab has adapted previous techniques for removing the cortical tissue overlaying the DG and implanting of a titanium window with a glass coverslip above the intact hippocampus. Although this surgery technique is invasive as it removes the cortical tissue lying above the hippocampus, it has been shown that the cranial window preserves neurogenesis and cortical inputs into the DG. Furthermore, the mice are still able to complete DG-dependent context discrimination tasks (Goncalves et. al 2016).

Studies measuring calcium activity via two-photon imaging have used either a synthetic calcium-sensitive fluorescent indicator or genetically encoded calcium

indicator (Chen at al., 2013). Viral vectors are used to deliver genetically encoded calcium indicator into the target cells, resulting in expression of a protein complex composed of circularly permutated green fluorescence protein (cpGFP) with its C-terminus connected to calcium sensitive calmodulin (CaM) and its N-terminus connected to the CaM interacting peptide M13. In the presence of calcium, CaM undergoes a conformational change in the CaM-M13 complex, resulting in a subsequent change in cpGFP or other circularly permuted fluorescent protein that causes the chromophore to increase in brightness (Chen et al., 2013; Nakai et al., 2000). This type of indicator is useful to indirectly measure neuronal activity because presynaptic depolarization caused by action potentials causes the opening of voltage gated calcium channels resulting in the transient influx of calcium into the cell (Llinás, 1991; Murphy et al., 1995). These calcium transients allow for optical monitoring of activity within neurons (Chen et al., 2013; Murphy et al., 1995; Takechi et al., 1998). Previous studies have shown that this technique can accurately estimate both isolated and sequential action potentials (Greenberg et al., 2008). The development of a new generation of red-shifted genetically encoded Ca^{2+} indicators for monitoring neural activity allows us to image through deeper layers of the brain. Red calcium indicators have several advantages over green calcium indicators for deep tissue imaging. Red calcium indicators are excited by more red-shifted infra-red light compared to their green fluorescent counterparts. The fluorescence from green calcium indicators also have increased absorption by hemoglobin within the blood (Dana et al 2014).

In this study, we will be using the chronic pilocarpine murine model, which emulates the clinical and pathological features of human mTLE. In patients, mTLE is thought to be initiated by lesions and functional alterations secondary to a variety of injuries such as febrile convulsions, encephalitis, or trauma, which after a 5 to 10 year latency period generate spontaneous motor seizures (Engel 1993). Pilocarpine is a muscarininc cholinergic agonist that causes an imbalance between excitatory and inhibitory transmission resulting in SE (Priel and Albuquerque 2002). An initial precipitating injury in the form of pilocarpine induced status epilepticus (SE) is followed by a latent seizure-free period, and subsequent spontaneous recurrent temporal lobe seizures in rodents (Leite et al. 1990) (Cavalheiro et al. 1991). Hippocampal sclerosis and neuronal network reorganization such as aberrant newborn DGC migration, and mossy fiber sprouting are key pathological features in this model (Wieser 2004).

Chapter 2. Materials and Methods

Induction of temporal lobe epilepsy in Mice

Male C57BL/6 mice were obtained from Charles River Laboratories. The mice were kept in standard regular cages with at most five mice in one cage on a 12-hour light/dark cycle. Pilocarpine induction was performed on the mice when they reached 6 weeks old. Mice were administered an intraperitoneal injection (ip) of 1mg/kg of N-methylscopolamine bromide 30 min prior to injection of pilocarpine hydrochloride to reduce peripheral cholingergic effects (Mazzuferi et al. 2012). A single dose of pilocarpine was administered based on the weight of each mouse. A pilocarpine dosage of 250mg/kg was administered on mice that weighed more than 25g. A pilocarpine dosage of 275mg/kg was administered on mice that weighed between 20 and 25g. A pilocarpine dosage of 285mg/kg was administered to mice that weighed less than 20g. The mice were monitored for behavioral seizures. Subsequent pilocarpine doses were administered 45min to an hour after a mouse's last seizure if they had not entered SE yet. After 2 hours of sustained seizures in the mice that developed SE, the mice were then administered diazepam (10mg/kg) to attenuate seizure activity and re-administered after 30 to 40 minutes if seizure activity persisted. The mice were then given 1cc of saline IP to compensate for lost body fluids during SE. Control mice received identical injections, except for saline instead of pilocarpine. Animal use and protocols were approved by the University of California San Diego

Institutional Animal Care and Use Committee and the Salk Institute Animal Care and Use Committee.

Adenovirus Labeling of Dentate Granule Neurons

Dentate granule cells were injected with an attenuated adenovirus expressing a red fluorescent Calcium dye under the control of the calcium/calmodulin-dependent kinase-α promoter (AAV8 CaMKIIα::jRGECO1α). For the surgery, the mice were anesthetized with 5% isoflurane and kept under 1.5% isoflurane (0.5L/min in O_2). The hair on the mouse's head was shaved to avoid contamination of the surgical site. The mice were fixed onto a stereotaxic surgery rig (Stoelting, Wood Dale, IL) on a 37° C water-circulating blanket to keep the mouse's body temperature stable. PuraLube opthalamic ointment (Dechra Pharmaceuticals PLC, Northwhich, England) was administered to the mouse's eyes. The surgical site was cleaned three times by rotating applications of 10% povidone-iodine (Dynarex, Orangeburg, NY) and 70% ethanol. With a scalpel, a 2cm incision was made. 1ul of AAV was injected into the right hemisphere by stereotaxic techniques. The coordinates used to locate the dentate gyrus were calculated by measuring the distance between bregma and lambda in the anteroposterior (A/P) plane as described before (Zhao et. al 2006). For CA1 injections, the coordinates were measured using the same anterior/posterior movement and same lateral movement with the dorsal/ventral movement of the needle being 1.37mm. For CA3 injections, the coordinates were taken from bregma, with an anterior/posterior movement of -1.8mm, a lateral movement of -1.8mm, and a dorsal/ventral movement of -2.2mm. A pneumatic dental drill was used to create a hole in the skull (Midwest

Traidition, DentSply, York, PA). The virus was injected using a Nanoject II Auto-Nanoliter Injector (Drummond Science, Broomall, PA) and a pulled glass capillary tube in 23 nL pulses in 10 second intervals for a total of 7.5min (1.035 uL total). After 7.5 min, the nanoinjector was left inside the skull for seven minutes to allow for the viral suspension to diffuse. The injection capillary was then slowly removed, and the incision was closed using cyanoacrylate adhesive. Mice were given carprofen (5mg/kg) to reduce inflammation.

Table 1. Measurements for Determining Dentate Granule Injection Site

Half distance between lambda and bregma (mm)	Anterior/Posterior movement of needle (mm)	Lateral movement of needle (mm)	Dorsoventral movement of needle (mm)
1.50	-1.50	-1.50	-1.80
1.60	-1.60	-1.55	-1.80
1.70	-1.70	-1.60	-1.90
1.80	-1.80	-1.65	-1.90
1.90	-1.90	-1.70	-2.00
2.00	-2.00	-1.75	-2.00

A titanium cranial window implant with a #1 glass coverslip (diameter: 3mm; depth: 1.3mm) was embedded into the brain above the CA1. The viral injection and window surgery were performed on the same day. For the surgery, the mice anesthetized with 5% isoflurane and mice were kept under 1.5% isoflurane (0.5L/min in O_2). Dexamethazone (2.5 mg/kg, I.P.; Butler Schein Animal Health, Dublin, OH) was given prior to surgery to reduce tissue swelling. The mice were fixed onto a stereotaxic surgery rig (Stoelting, Wood Dale, IL) on a 37° C water-circulating blanket to keep the mouse's body temperature stable. PuraLube opthalamic ointment (Dechra Pharmaceuticals PLC, Northwhich, England) was administered to the mouse's eyes.

The surgical site was cleaned three times by rotating applications of 10% povidone-iodine (Dynarex, Orangeburg, NY) and 70% ethanol. The scalp was cut and discarded to expose the dorsal surface of the skull and underlying connective tissue. The skull was wiped with sterile cotton-tipped applicators. Two coats of OptiBond All-In-One dental adhesive (Kerr Corporation, Orange, CA) were administered to the skull and UV cured for 60 seconds. Using a standard pneumatic dental drill (Midwest Tradition, DentSply, York, PA), a 3mm diameter circle of skull was removed from the right hemisphere above the coordinates for the DG previously obtained from the viral injection surgery, and the underlying dura mater was removed with a #11 scalpel. The cortex below the lesion was aspirated using a blunt tip 25-gauge needle (Grainger, Lake Forest, IL) attached to a vacuum line until CA1 was reached. The surgery was irrigated periodically with sterile saline to nurse the lesion, reduce bleeding, and prevent blood clotting. When the bleeding had stopped, the titanium window was implanted onto the surface of CA1 and attached to the skull with two applications of OptiBond All-In-One dental adhesive (Kerr Corporation, Orange, CA) and UV cured. A thin layer of fast curing orthodontic acrylic resin (Lang Dental Mfg., Wheeling, IL) was applied over the surface of the skull to close over the exposed surface of the skull and reinforce the window's attachment. A titanium head bar was secured adjacent to the implant using a second layer of orthodontic acrylic to allow for fixing of the head in future imaging sessions. Following completion of the surgery carprofen (5 mg/kg, I.P.) and buprenorphine (0.05-0.1 mg/kg, S.Q.) were respectively administered for inflammation and analgesic relief.

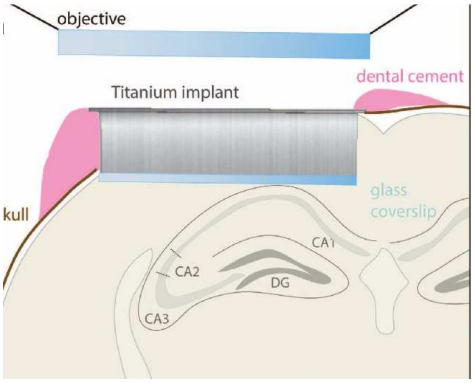

Figure 2. Cranial Window Surgery. The tissue above the hippocampus is aspirated, allowing implantation of a titanium window with a 3mm #1 glass coverslip. This surgery allows 2-photon imaging of deeper tissue layers. This surgery was adapted from Goncalves et. al 2016.

2-photon Imaging of DG

For imaging, the mice were head-fixed on a cylindrical treadmill equipped with motion tracking. Imaging was performed using a 2-photon laser-scanning microscope (Movable Objective Microscope; Sutter Instruments, Novato, CA), equipped with a tunable femtosecond-pulsed titanium-sapphire laser (Chameleon Ultra II, Coherent, Santa Clara, CA), fixed wavelength 1050 nm femtosecond-pulsed fiber laser (Fidelity II, Coherent, Santa Clara, CA), and a 16x water immersion objective (0.8 NA, Nikon). Movies were acquired using the ScanImage software (Pologruto et al., 2003), which was written in MATLAB (MathWorks). Selected regions of the DG expressing jRGECO1a were imaged at λ_{ex} = 1050 nm and high-resolution videos (512 x 128 pixels; frame rate 3.91 Hz) were obtained at 9, 11, 13, and 17 dpi. Simultaneously during video acquisition, motion tracking data were also recorded. A motion sensor

was attached to the treadmill, to track mouse movement. The signal was digitized using a multichannel A/D converter Digidata 1440 interface (Molecular Devices) coupled to a computer running WinWCP V5.1.5 software (University of Strathclyde Faculty of Science).

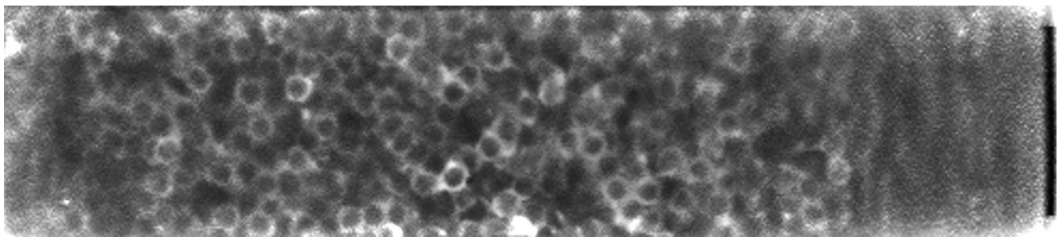

Figure 3. Single frame of 2-photon calcium imaging. Snapshot of frame taken during imaging sessions.

Tissue Preparation and Immunohistochemistry

Mice were anesthetized with a lethal dose of Ketamine/Xylazine (130mg/kg, 15mg/kg; I.P) and perfused transcardially with 0.9% NaCl followed by 4% paraformaldehyde (PFA) in 0.1M phosphate buffer (pH 7.4). Brains were dissected and postfixed in 4% PFA overnight and transferred to a 30% sucrose solution for 24-72 hours to equilibrate. Fixed, frozen brains were sectioned coronally at 40 μm thickness on a sliding microtome, and sections were stored individually in a 96-well plate in tissue cryogenic solution (TCS) (23.8% glycerol, 28.6% ethylene glycol, 47.6% 0.1 M phosphate buffer (v/v)). Brain sections of one-in-twelve or one-in-six series were selected for immunostaining (Table 2) and/or 4',6-diamidino-2-phenylindole (DAPI) staining to identify nuclei. Brain slices were rinsed in TBS and mounted on double subbed slides with polyvinyl alcohol (PVA) mounting medium with DABCO (Sigma). Fluorescence was detected using an Olympus confocal

microscope and images were processed using Fiji, Adobe Photoshop CS3 (Adobe Systems), and Adobe Illustrator CS3 (Adobe Systems).

Table 2. Antibodies used for histological analysis

Antigen	Host	Type	Provider	Dilution
Doublecortin (DCX)	Goat	Polyclonal	Santa Cruz Biotechnology	1:250
Allograft inflammatory factor 1 (Iba 1)	Rabbit	Polyclonal	Wako	1:500
Goat IgG	Donkey	Cy5-conj.	Jackson IR	1:250
Rabbit IgG	Donkey	AF 647-conj.	Jackson IR	1:250

Data Analysis

The motion tracking data and the movies were processed using four subroutines written in MATLAB (Mathworks) for motion detection, motion correction, segmentation, and data analysis. The code written in MATLAB (Mathworks) was developed by Alexander Newberry at the Gage Lab and Dr. Ondre Novak of Palacky University Olomouc. The code constructs reference frame by averaging the most stable frames of the video. A stabilization algorithm assigns each frame a correlation coefficient, removing any frame that does not reach a certain stabilization threshold (Fig. S1). The remaining frames are motion corrected through maximization of the correlation coefficient with the reference frame by adjusting the position of rows and columns in the frame. Once the movie has been motion corrected, each individual cell

is identified (segmentation) and analyzed for its brightness over time (ΔF/F data) (Fig. S2 and Fig. S3). In order to quantify the level of spontaneous network activity, we used primarily two metrics of excitability the percentage of active cells per field of view (% active cells), where active cells are defined as having at least one response (fluorescence fluctuations [ΔF/F] with amplitude > 5 SD above background noise), and 2) the mean Ca2+ activity per active cell ([ΔF/F]active = [integrated ΔF/F]/time). Finally synchronous activity was examined where the average amplitude of pairwise cross-correlations between neurons i and j will be calculated as a function of lag time τ ($G_{ij}(\tau) = \frac{1}{T}\int_0^T \frac{\Delta F_i(t)\Delta F_j(t+\tau)}{\langle \Delta F_i \Delta F_i \rangle} dt$) and distance δ ($G_{ij}(\delta) = \frac{1}{R}\int_0^R \frac{\Delta F_i(r)\Delta F_j(r+\delta)}{\langle \Delta F_i \Delta F_i \rangle} dr$) (Shtrahman et al) (Smedler et al).

Chapter 3 Results

AAV titer concentration reduces neurogenesis

1ul of recombinant adenovirus expressing a red fluorescent Calcium dye under the control of the calcium/calmodulin-dependent kinase-α promoter (AAV8 CaMKIIα::jRGECO1α) was injected unilaterally into wild-type C57Bl6 to label excitatory cells through stereotaxic surgery (Zhao et. al 2006). Three cohorts of mice with 4 mice each received either an adenovirus titer concentration of 1.5 E11, 5 E11, or 1.5 E12. The cranial window surgery was performed on each mouse, and these mice were imaged under the 2-photon microscope on 9,11, 13, 17, and 21 days post injection. Due to the depth at which the DG is located, conventional fluorescence-based imaging modalities would be unable to image the GFP+ granule neurons which lie ~1.7mm below the surface of the cortex. To circumvent this issue, a small craniotomy (3mm) was created in the skull and parts of the underlying cortex and corpus callosum were removed in order to place a chronic imaging window above the surface of the DG, which remained intact (Fig. 2). After injection of the virus and placement of the window implant, mice were returned to their home cage to recover. Detecting a signal in-vivo required a long time for expression and buildup of adequate jRGECO levels. Mice were not imaged on consecutive days to avoid excess power and heat being applied to the brain. Using the center of the cranial window as the origin, a coordinate system was created to identify the same regions in the DG from

different imaging session days. 5-minute videos recording the activity were taken and then analyzed via code written in MATLAB.

During calcium imaging, it was observed that the activity in the DG was affected by the virus titer concentration used. The mice injected with the low titer of 1.5 E11 had more activity observed than the mice injected with the high titer of 1.5 E12. After imaging was concluded on day 21, the mice were perfused for histological analysis. Doublecortin (DCX) is a microtubule-associated protein almost expressed by NPCs and immature neurons during the first 2-3 weeks of their development (Francis et al., 1999). Because of this it is very commonly used as a marker of neurogenesis (Piatti et al., 2006; Gleeson et al., 1999). The mice injected with the highest titer of 5 E12 expressed lower levels of neurogenesis compared to the mice injected with the lower titers as seen by the DCX stain results (Fig. 4). The stain results combined with the observations from the imaging sessions indicate that the decrease in neurogenesis that results from a high titer of adenovirus causes a decrease in the excitability of the hippocampus.

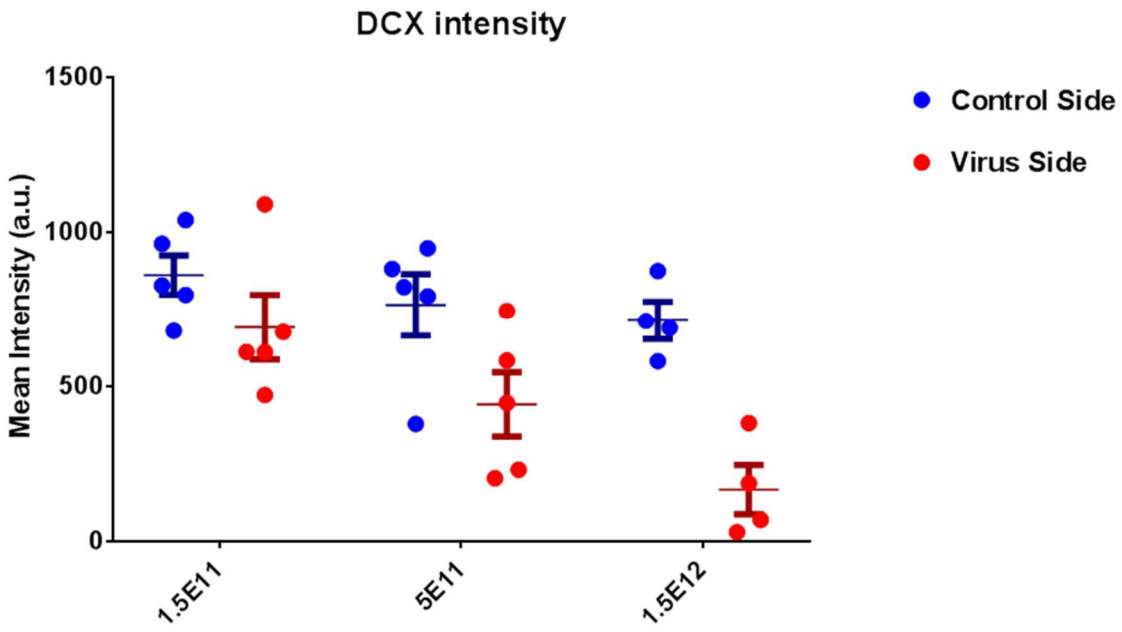

Figure 4: AAV-jRGECO1a titer concentration affects neurogenesis. 3 cohorts of mice were injected with varying titer concentrations. The mean intensity of the DCX is inversely related to the concentration of the virus.

Injecting FLEX.AAV.jRGECO1a into WT animals reduces neurogenesis

1ul of a FLEX.AAV.jRGECO1a was injected unilaterally into wild-type C57Bl6 in order to investigate whether the knockdown of neurogenesis was a result of the high protein expression. The strategy used in this experiment is the flip-excision (FLEX) switch, which utilizes Cre-dependent transgene inversion (Atasoy et al. 2008). In the absence of Cre, the transgene, in this case the jRGECO1a, is inverted with respect to the promoter, preventing protein expression. Injection of the FLEX.AAV.jRGECO1a at two different titer concentrations would infect excitatory cells in the DG but not allow for expression of the calcium indicator. We hypothesized that if the infection of immature DGCs resulted in their death, then we should observe little to no loss of these immature DGCs in these mice injected with the FLEX.AAV.jRGECO1a. One

cohort of mice received the injection with a titer of 5 E12 while another cohort of mice received the injection with a titer of 5 E11. These mice were perfused, and histological analysis was performed on these mice. Injection of the high titer of 5 E12 resulted in complete loss of DCX cells on the injected side, while the contralateral (control) side remained intact (Fig. 5a, 5b). Injection of the low titer of 5 E11 resulted in some loss of DCX cells compared to the contralateral side (Fig. 5c, 5d). Additionally, increased expression of ionized calcium binding adaptor molecule 1 (Iba1) throughout the hippocampus was also often observed. Iba1 is a calcium binding protein that is specifically expressed in activated microglia following neural injury (Ito et al., 1998), used here as an indirect marker of inflammation. As indicated by the stain, the inflammation was inconsistent throughout these mice. We thought that the expression of the fluorescent calcium indicator may actually be toxic to these immature DGCs or overwhelming the cells' synthetic machinery resulting in their death. However through this experiment, we were able to reproduce the loss of neurogenesis with the FLEX.AAV.jRGECO1a, indicating that the death of newborn cells is due to the higher concentration of virus and is independent of protein expression.

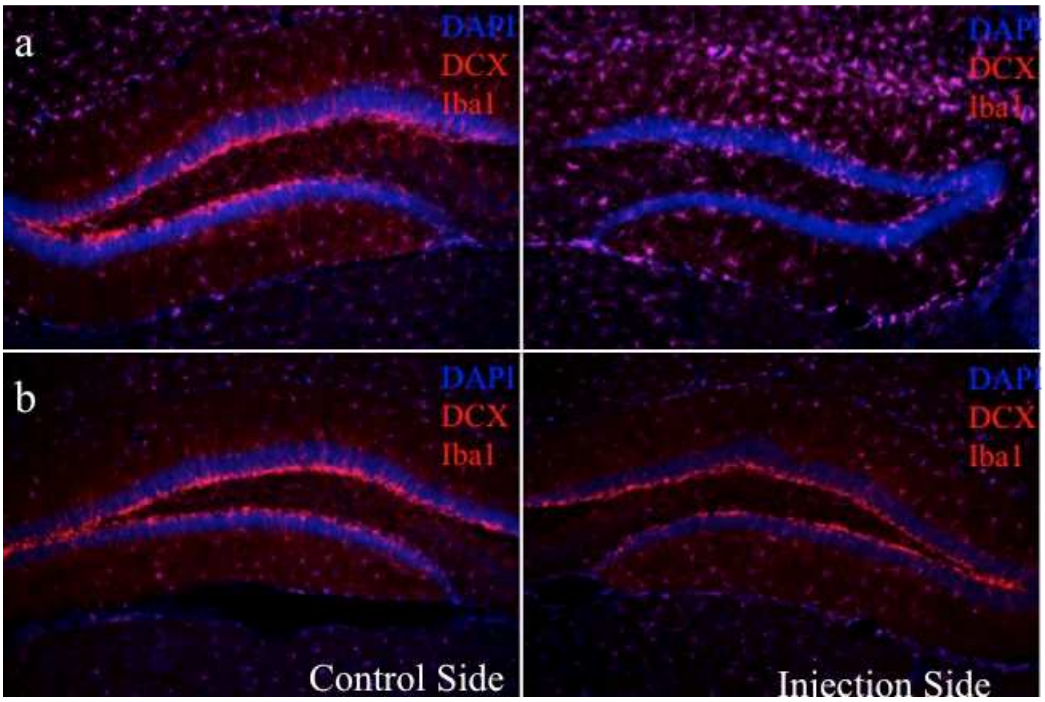

Figure 5: Injection of high titer Flex-AAV jRGECO1a knocks out neurogenesis. 3a) The contralateral side of the flex-AAV high titer injection is unaffected by the unilateral viral injection 3b) The DCX stain is decreased even though there is no protein expression of the jRGECO1a. 3c) The contralateral side of the flexed-AAV low titer injection has normal amounts of DCX expression 3d) The injection side has some loss of DCX cells compared to the control side.

Imaging of the dentate gate hypothesis in epileptic mice

In this study, mice were induced with pilocarpine to emulate the key features of mTLE. Control literrmate mice received identical injections with saline given instead of pilocarpine. Experimental mice that entered status epilepticus, the initial precipitating injury for epilepsy were kept in the animal vivarium for 10 weeks before viral injection. Studies using Ki-67, a marker for endogeneous cell proliferation marker, and short-pulse bromodeoxyuridine (BrdU) mitotic labeling have shown that the DG increases cell proliferation in the subgranular zone after status epilepticus (SE)

(Jessberger et al. 2005) (Parent et. al 1997). This dentate gyrus cell proliferation increases 5-10 fold after a latent period of several days and persists for several weeks before returning to baseline levels (Parent et. al 1997). For AAV labeling of the DGCs, a titer concentration of 1.5 E11 was used to avoid killing newborn DGCs.

We hypothesized that damage to the brain via pilocarpine induction of status epilepticus would impair the dentate gate ability to regulate activity and result in a hyperexcitable DG. During imaging sessions, the DG of epileptic mice were observed to have much more activity than the DG of control mice. After data analysis of the videos recorded, we looked at the average calcium fluctuations of the cells in the videos. Higher calcium fluctuations were observed in the epileptic animals. The average behavior of the network in the epileptic mice also seemed to show oscillations where activity would ramp up over X seconds and then reset (Figure 6). In the future, simultaneously monitoring EEG recordings and field potentials while imaging for calcium activity will provide more insight into this ramping behavior observed in the epileptic animals. Furthermore, in the epileptic mice, we observed bursts of flashes where multiple cells would fire at the same time, indicating a level of synchrony in the epileptic brain after putative loss of the dentate gate (Fig. 7).

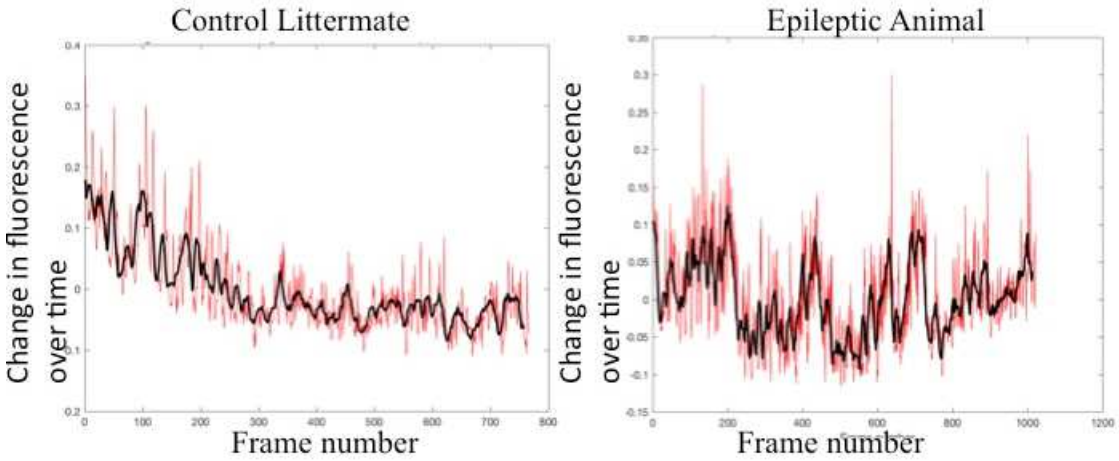

Figure 6: Epileptic mice have higher calcium fluctuations. a) Average fluorescent intensity of the cells in the control mice b) Average fluorescent intensity of the cells in the epileptic mice

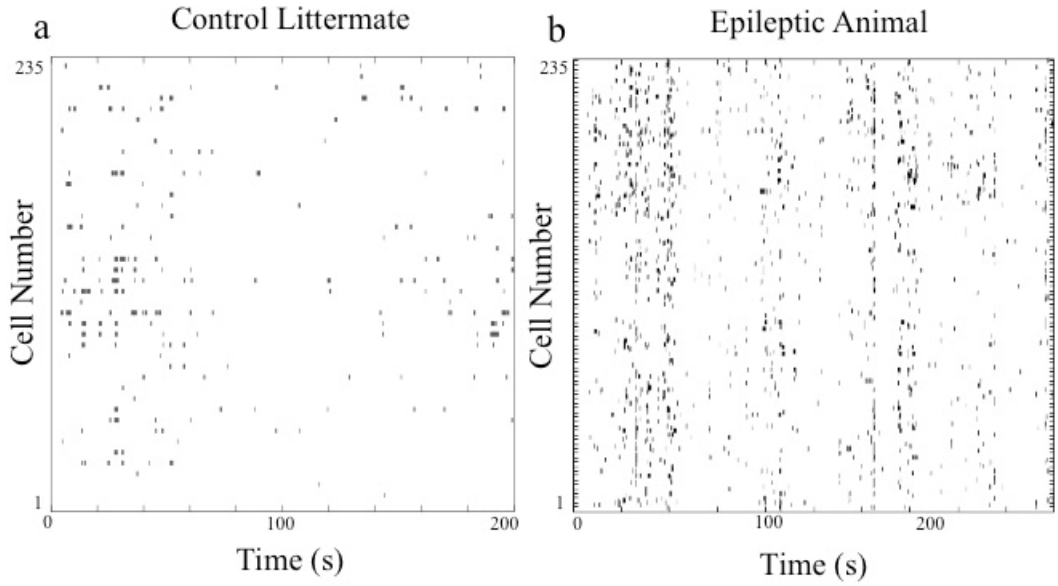

Figure 8: Raster plots showing synchronous and hyperexcitable firing. Short vertical dashes represent when each cell exceeds arbitrary calcium threshold. Raster plot of activity in a) control mouse and b) epileptic animal. Note epileptic animal shows marked hyperexcitability and synchronous firing events.

2-photon imaging using retroAAV vector

There were difficulties observed in the experiment with many mice, both control and epileptic mice, showing low quality imaging data. We hypothesized that this could be due to the effects of high AAV titer on neurogenesis levels and activity in the DG in general. To circumvent this issue, we used another approach with a retrograde adeno-associated viral vector (rAAV-retro) under the control of the CamKIIa promoter. The rAAV-retro retrogradely transduces projection neurons after injection at the site of the axon terminals (Cook-Snyder et. al 2015). Utilizing the brain's projections and connectivity with other neurons such as the tri-synaptic circuit, we injected the rAAV.jRGECO1a into CA3, allowing for the red calcium indicator to become concentrated into the DGCs through retrograde transport. Preliminary data with this technique has yielded 5 mice with successful imaging session.

The videos taken of the DG in the epileptic mice injected with the rAAV-retro did not seem to show a hyperexcitable nature compared to the control mice. Data analysis performed on the mice looked at the fluorescent changes, synchronous firing, and number of cells firing. Compared to the control mice, the epileptic animals did not show higher fluctuations in calcium activity, but did exhibit the same network behavior observed in the epileptic animals injected with the normal rAAV.jRGECO1a approach (Fig. 8). The synchronous firing events were observed in the epileptic mice injected compared to controls with the rAAV-retro approach, as seen in the raster plot (Fig. 9). From observations, it seems that there is less synchronous firing events in the

epileptic mice injected with the rAAV-retro that with the standard approach, but we will need additional experiments to verify these differences.

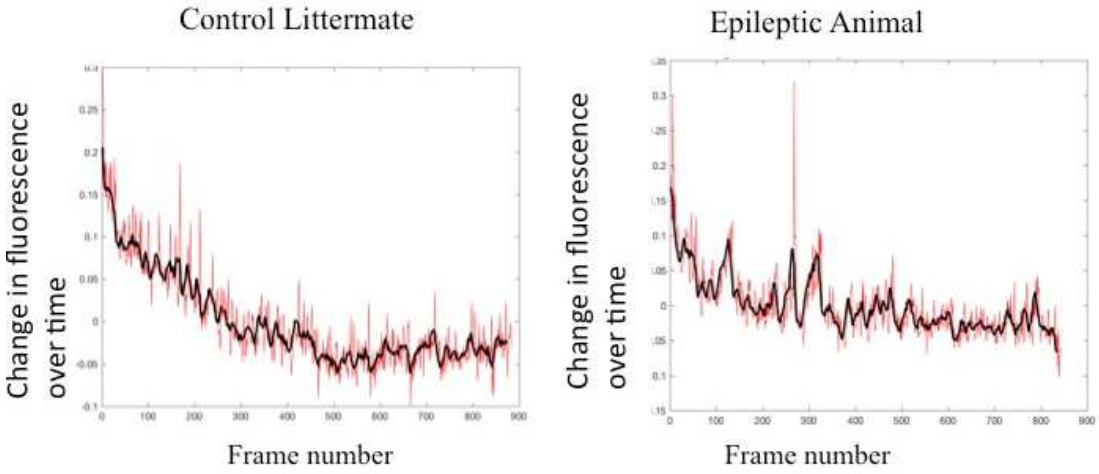

Figure 10: Ramping behavior observed in the rAAV-retro approach. a) Average fluorescent intensity of the cells in the control mice b) Average fluorescent intensity of the cells in the epileptic mice

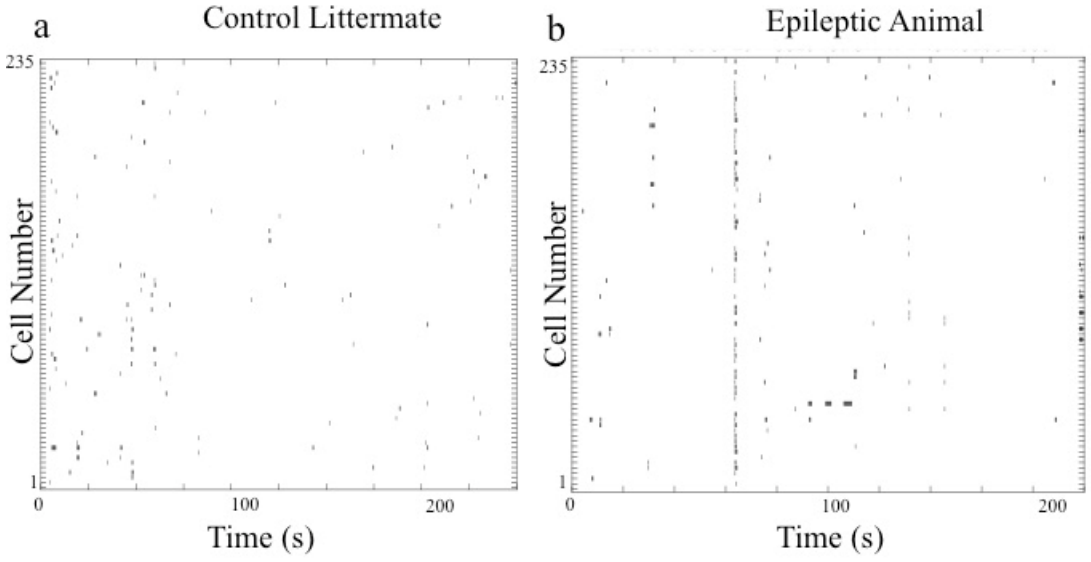

Figure 9: Raster plots showing synchronous firing in the rAAV-retro approach. Short vertical dashes represent when each cell exceeds arbitrary calcium threshold. Raster plot of activity in a) control mouse and b) epileptic animal. Note epileptic animal shows synchronous firing events.

Chapter 4 Discussion

The dentate gate hypothesis is not completely accepted as there are discrepancies in the research. Optogenetics studies have provided in vivo evidence that DG activation is necessary for seizure propagation in mTLE (Krrok-Magnuson et al 2015). In contrast, electrophysiology experiments have shown that synaptic inputs from the EC in rat models of mTLE cause hyperexcitability in CA1 cells and not the DGCs (Ang et al 2006) (Coulter et al 2011). In this study, we have in vivo data obtained that is consistent with hyperexcitability of the DG in a mouse model of mTLE. The DG in the epileptic mice displayed synchronous firing as seen by the flashes, marked hyperexcitability, and higher calcium fluctuations. Further experiments will be needed to confirm this result. Many cohorts of mice were injected with AAV.CamKII.jRGECO1a and were not imageable at all. Out of every cohort of 8 mice, around 0-1 mice would have successful imaging results. This low level of success is not seen when imaging 8-week-old control mice. Possible reasons to explain the lack of good imaging results may be because of inflammation that could have been developed from the surgeries that is precluding imaging. Another possibility is that the quality of imaging is dependent on whether the injection successfully reaches the upper blade of the DG as opposed to the bottom blade. Because of the inherent variability in the pilocarpine model (Curia et. al 2008) and without more data samples, it is difficult to conclude whether the differences between the two approaches is due to differences in the mice or the approach itself.

Furthermore in this study, we discovered that the titer of the AAV directly affects neurogenesis. A higher titer concentration of virus ablates neurogenesis. Initially, we hypothesized that the death of immature DGCs was due to high protein expression of the genetically encoded calcium indicator. Perhaps the production of this calcium indicator was toxic to the immature DGCs or overwhelmed the cells' synthetic machinery. Injection of the flexed-AAV jRGECO1a reproduced the loss of immature of DGCs without protein expression. These experiments point to a possible solution of injecting AAV at a low titer and using a strong promoter system to increase protein expression to allow for good imaging. One potential solution could be to generate AAV vectors that use a positive feedback loop made of a Tet promoter driving both its own tetracycline-dependent transcription activator (tTA) and the jRGECO1a. This positive transcriptional feedback loop (TLoop) has been successfully generated in lentiviral vectors, allowing for high levels of gene expression even with inefficient viral transduction (Cetin et. al 2014). Optimizing the 2-photon imaging with the rAAV-retro seems to be the most promising solution. Lastly, the ablation of neurogenesis by using a high titer of virus suggests that AAV may be used as a tool for focal knockdown of neurogenesis that could be used in conjunction with the evoked experiments and helping understand the role of these newborn neurons.

Future Directions:

Once the approach is successfully optimized and mice can consistently be imaged well, we will begin the next set of experiments. We are looking to develop statistical measures of synchrony so we can compare the level of synchrony between epileptic

and control mice. We will simultaneously monitor EEG recordings and field potentials while imaging for calcium activity so we can monitor for seizure activity and provide more insight into the flashes. After having looked at the spontaneous activity of the DG in epileptic mice, we will also begin looking at the evoked responses, using electrodes to stimulate the perforant pathway, to see if evoked responses also demonstrate hyperexcitability. This will provide further insight into the dentate gate hypothesis.

Once we have obtained more data about the dentate gate hypothesis, we will then move onto elucidating the role of adult-born immature DGCs in epileptogenesis. Previous studies using retroviral labeling of DGCs in combination with low-dose irradiation to suppress DGC neurogenesis showed that neither neonatal born DGCs nor those born after SE contributed to mossy fiber sprouting. Only DGCs that were 2-4 weeks old at the time of SE showed aberrant axonal reorganization (Kron et. al 2010). In the videos of the epileptic mice, we also saw in the molecular layer above the DG structures that may represent mossy fiber boutons. In patients with temporal lobe epilepsy, Golgi-stained mossy fibers projected through the granule cell layer and into the molecular layer where their boutons synapsed onto granule cell dendrites (Scheibel et al 1974). Using RV-CAG-EGFP to infect these dividing cells after SE and in vivo 2-photon imaging will help us understand whether immature adult-born DGCs or mature adult-born DGCs contribute to the hyperexcitability observed during epileptogenesis.

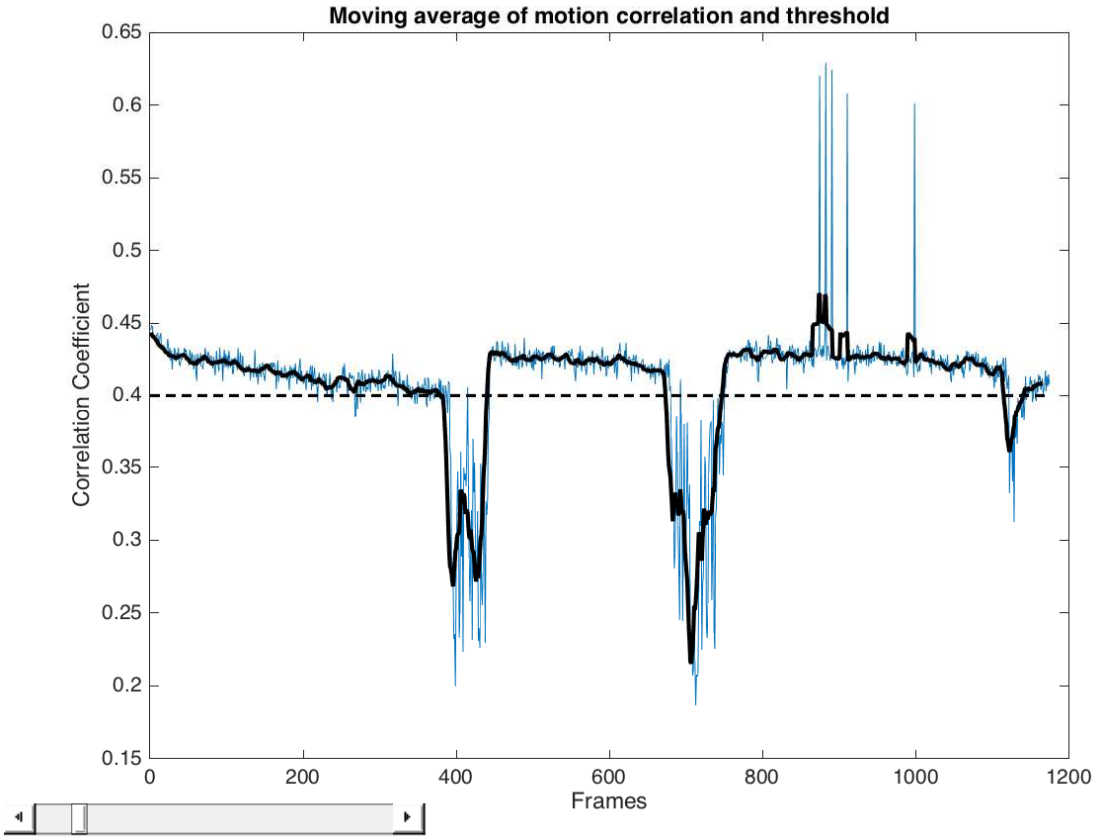

Supplementary Figure S1. **MATLAB motion correction analysis.** Plot of movement data obtained before the 5 minute videos are processed through the motion correction code.

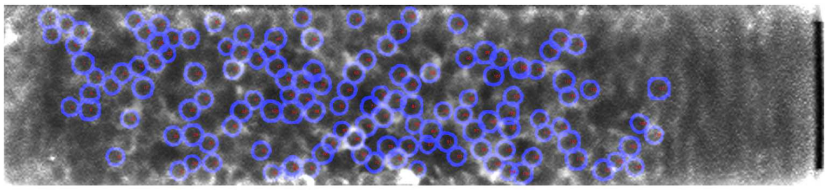

Supplementary Figure S2. MATLAB segmentation analysis. Results of the segmentation code, highlighting individual cells and recording their individual activity

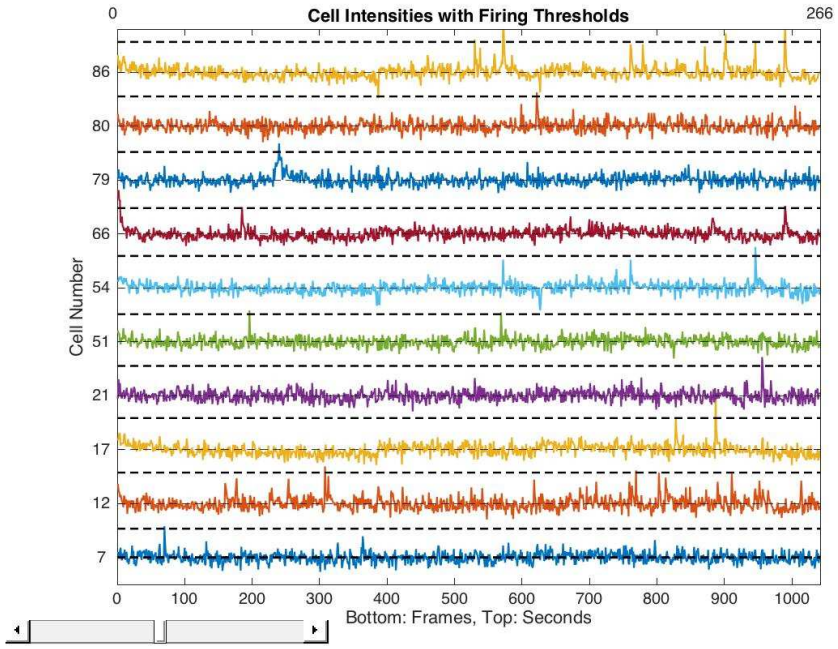

Supplementary Figure S3. MATLAB Data Analysis. A plot obtained after the data analysis code, with a firing threshold labeled to identify which cells are firing and which are not

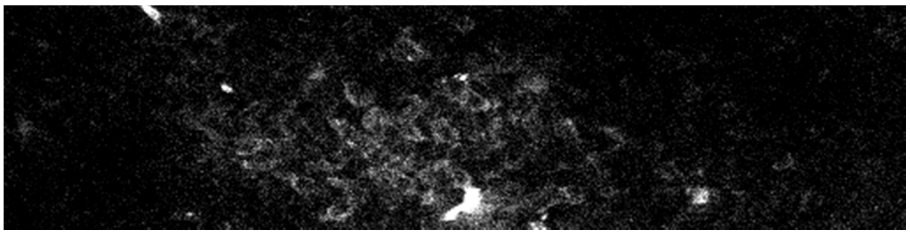

Supplementary Figure S4. Mossy bouton visualized. A single frame taken in the video of an epileptic mouse, about 10-20um above the DG in the molecular layer, that seems to be a mossy fiber bouton

References

Ang, C. W., Gc, C. & Coulter, D. A. Massive and specific dysregulation of direct cortical input to the hippocampus in temporal lobe epilepsy. Journal of Neuroscience 26 (2006).

Atasoy D, Aponte Y, Su HH, Sternson SM. A FLEX switch targets Channelrhodopsin-2 to multiple cell types for imaging and long-range circuit mapping. The Journal of neuroscience : the official journal of the Society for Neuroscience. 2008;28(28):7025-7030. doi:10.1523/JNEUROSCI.1954-08.2008.

Babb TL, Kupfer WR, Pretorius JK, Crandall PH, Levesque MF. Synaptic reorganization by mossy fibers in human epileptic fascia dentata. Neuroscience. 1991;42(2):351–363

Buckmaster, P. S. & Lew, F. H. Rapamycin Suppresses Mossy Fiber Sprouting But Not Seizure Frequency in a Mouse Model of Temporal Lobe Epilepsy. The Journal of Neuroscience 31, 2337-2347, doi:10.1523/jneurosci.4852-10.2011 (2011).

Cavalheiro EA, Leite JP, Bortolotto ZA, Turski WA, Ikonomidou C, Turski L. Long-term effects of pilocarpine in rats: structural damage of the brain triggers kindling and spontaneous recurrent seizures. Epilepsia 1991;32:778–82.

Cetin A, Callaway EM. Optical control of retrogradely infected neurons using drug-regulated "TLoop" lentiviral vectors. Journal of Neurophysiology. 2014;111(10):2150-2159. doi:10.1152/jn.00495.2013.

Chawla M. K., Guzowski J. F., Ramirez-Amaya V., Lipa P., Hoffman K. L., Marriott L. K., et al. (2005). Sparse, environmentally selective expression of Arc RNA in the upper blade of the rodent fascia dentata by brief spatial experience. Hippocampus 15, 579–586 10.1002/hipo.20091

Chen T.W., Wardill T.J., Sun Y, Pulver S.R., Renninger S.L., Baohan A, Schreiter E.R., Kerr R.A., Orger M.B., Jayaraman V., Looger L.L., Svoboda K, Kim D.S. Ultrasensitive fluorescent proteins for imaging neuronal activity. Nature. 2013 Jul 18;499(7458):295-300..

Coulter, D. A., C, Y., Ang, C. W., Weissinger, F., Goldberg, E., Hsu, F.-C., Carlson, G. C. & Takano, H. Hippocampal microcircuit dynamics probed using optical imaging approaches. (2011).

Curia G, Longo D, Biagini G, Jones RSG, Avoli M. The pilocarpine model of temporal lobe epilepsy. Journal of Neuroscience Methods. 2008;172(2-4):143-157. doi:10.1016/j.jneumeth.2008.04.019.

Curtis, Maurice A. et al. "Human Neuroblasts Migrate to the Olfactory Bulb via a Lateral Ventricular Extension." *Science (New York, N.Y.)* 315.5816 (2007): 1243–1249. *NCBI PubMed*. Web.

Dana, H., Sun, Y., Hasseman, J. P., Tsegaye, G., Holt, G. T., Fosque, B. F., Schreiter, E. R., Brenowitz, S. D., Jayaraman, V., Looge, L. L., Svoboda, K. & Kim, D. S. Improved red protein indicators for in vivo calcium imaging (Society for Neuroscience 2014).

deAlmeida L, Idiart M & Lisman JE (2009). The input–output transformation of the hippocampal granule cells: from grid cells to place fields. J Neurosci 29, 7504–7512.

Denk, W., J. H. Strickler, and W. W. Webb. "Two-Photon Laser Scanning Fluorescence Microscopy." *Science (New York, N.Y.)* 248.4951 (1990): 73–76. Print.

Deng, W., Aimone, J. B. & Gage, F. H. New neurons and new memories: how does adult hippocampal neurogenesis affect learning and memory? Nat Rev Neurosci 11, 339-350, doi:http://www.nature.com/nrn/journal/v11/n5/suppinfo/nrn2822_S1.html (2010).

Devinsky O. Diagnosis and treatment of temporal lobe epilepsy. Rev Neurol Dis. 2004 Winter;1(1):2-9.

Engel, J. Mesial Temporal Lobe Epilepsy: What Have We Learned? The Neuroscientist 7, 340-352, doi:10.1177/107385840100700410 (2001).

Engel, J., Jr. Update on surgical treatment of the epilepsies. Summary of the Second International Palm Desert Conference on the Surgical Treatment of the Epilepsies (1992). Neurology 43, 1612–7.

Francis F, Koulakoff A, Boucher D, Chafey P, Schaar B, Vinet M-C, Friocourt G, McDonnell N, Reiner O, Kahn A, McConnell SK, Berwald-Netter Y, Denoulet P, Chelly J (1999) Doublecortin is a developmentally regulated, mictrotubule-associated protein expressed in migrating and differentiating neurons. Neuron 23:247-256.

Gleeson, J. G. et al. "Doublecortin Is a Microtubule-Associated Protein and Is Expressed Widely by Migrating Neurons." Neuron 23.2 (1999): 257–271. Print.

Goncalves, Tiago, Cooper Bloyd, Matthew Shtrahman, Stephen Johnston, Simon Schafer, Sarah Parylak, Thanh Tran, Tina Chang, and Fred Gage. "In Vivo Imaging of

Dendritic Pruning in Dentate Granule Cells."Nature Neuroscience 19 (2016): 788-91. Pubmed. Web

Greenberg D.S., Houweling A.R., Kerr J.N. Population imaging of ongoing neuronal activity in the visual cortex of awake rats. Nat Neurosci. 2008 Jul;11(7):749-51. doi: 10.1038/nn.2140. Epub 2008 Jun 15.

Hattiangady B, Rao MS, Shetty AK. Chronic temporal lobe epilepsy is associated with severely declined dentate neurogenesis in the adult hippocampus. Neurobiol Dis. 2004 Dec;17(3):473–490.

Heinemann, U., H, B., Dreier, J. P., Ficker, E., Stabel, J. & Zhang, C. L. The dentate gyrus as a regulated gate for the propagation of epileptiform activity. Epilepsy Research, Supplemental 7 (1992).

Helmchen F., Denk W. Deep tissue two-photon microscopy. Nat Methods. 2005 Dec;2(12):932-40.

Houser, C. R. Do Structural Changes in GABA Neurons Give Rise to the Epileptic State? Advances in Experimental Medicine and Biology 813, 151-160 (2014).

Hunt, R. F., Km, G., Rubenstein, J. L., Alvarez-Buylla, A. & Baraban, S. C. GABA progenitors grafted into the adult epileptic brain control seizures and abnormal behavior. Nature Neuroscience (2013).

Ito, D. et al. "Microglia-Specific Localisation of a Novel Calcium Binding Protein, Iba1." Brain Research. Molecular Brain Research 57.1 (1998): 1–9. Print.

Jessberger S, Nakashima K, Clemenson GD Jr, Mejia E, Mathews E, Ure K, Ogawa S, Sinton CM, Gage FH, Hsieh J. Epigenetic modulation of seizure-induced neurogenesis and cognitive decline. J Neurosci. 2007 May 30;27(22):5967-75.

Jessberger S, Romer B, Babu H, Kempermann G. Seizures induce proliferation and dispersion of doublecortin-positive hippocampal progenitor cells. Exp Neurol. 2005 Dec;196(2):342–351.

Krook-Magnuson, E., Armstrong, C., Bui, A., Lew, S., Oijala, M. & Soltesz, I. In vivo evaluation of the dentate gate theory in epilepsy. The Journal of Physiology 593, 2379-2388, doi:10.1113/JP270056 (2015).

Leite JP, Bortolotto ZA, Cavalheiro EA. Spontaneous recurrent seizures in rats: an experimental model of partial epilepsy. Neurosci Biobehav Rev 1990;14:511–7.

Leutgeb JK, Leutgeb S, Moser MB & Moser EI (2007). Pattern separation in the dentate gyrus and CA3 of the hippocampus. Science 315, 961–966

Llinás R.R. Depolarization release coupling: an overview. Ann N Y Acad Sci. 1991;635:3-17.

Marin-Burgin, A., La, M., Pardi, M. B. & Schinder, A. F. Unique processing during a period of high excitation/inhibition balance in adult-born neurons. Science (2012).

Mathern GW, Leiphart JL, De Vera A, Adelson PD, Seki T, Neder L, et al. Seizures decrease postnatal neurogenesis and granule cell development in the human fascia dentata. Epilepsia. 2002;43(Suppl 5):68–73.

Mazzuferi M, Kumar G, Rospo C, Kaminski RM. "Rapid epileptogenesis in the mouse pilocarpine model: video-EEG, pharmacokinetic and histopathological characterization." *Exp Neurol*. 2012 Dec; 238(2):156-67.

McNaughton B.L., Morris R.G.M. Hippocampal synaptic enhancement and information storage within a distributed memory system. *Trends in Neurosciences*. 1987; 10(10):408-415

Murphy T.H., Baraban J.M., Wier W.G. Mapping miniature synaptic currents to single synapses using calcium imaging reveals heterogeneity in postsynaptic output. Neuron. 1995 Jul;15(1):159-68.

Moser, Edvard I., Emilio Kropff, and May-Britt Moser. "Place Cells, Grid Cells, and the Brain's Spatial Representation System." *Annual Review of Neuroscience* 31 (2008): 69–89. *NCBI PubMed*. Web.

Nakai J, Ohkura M, Imoto K. A high signal-to-noise Ca(2+) probe composed of a single green fluorescent protein. Nat Biotechnol. 2001 Feb;19(2):137-41.

O'Keefe J, Nadel L. The Hippocampus as a Cognitive Map Oxford University Press, New York (1978)

Parent J.M, Kron M.M. Neurogenesis and Epilepsy. In: Noebels JL, Avoli M, Rogawski MA, et al., editors. Jasper's Basic Mechanisms of the Epilepsies [Internet]. 4th edition. Bethesda (MD): National Center for Biotechnology Information (US); 2012.

Parent JM, Yu TW, Leibowitz RT, Geschwind DH, Sloviter RS, Lowenstein DH. Dentate granule cell neurogenesis is increased by seizures and contributes to aberrant network reorganization in the adult rat hippocampus. J Neurosci. 1997 May 15;17(10):3727–3738.

Peng Z, Houser CR. Temporal patterns of fos expression in the dentate gyrus after spontaneous seizures in a mouse model of temporal lobe epilepsy. J Neurosci. 2005;25:7210–7220.

Piatti, V. C., Ewell, L. A. & Leutgeb, J. K. Neurogenesis in the dentate gyrus: carrying the message or dictating the tone. Frontiers in Neuroscience 7, doi:10.3389/fnins.2013.00050 (2013).

Piatti, Verónica C., M. Soledad Espósito, and Alejandro F. Schinder. "The Timing of Neuronal Development in Adult Hippocampal Neurogenesis." The Neuroscientist: A Review Journal Bringing Neurobiology, Neurology and Psychiatry 12.6 (2006): 463–468. NCBI PubMed. Web.

Priel MR, Albuquerque EX. Short-term effect of pilocarpine on rat hippocampal neurons in culture. Epilepsia 2002;43(Suppl 5):40–6.

Scharfman, Helen E. "The CA3 'Backprojection' to the Dentate Gyrus." *Progress in Brain Research* 163 (2007): 627–637. *NCBI PubMed*. Web

Scheibel ME, Crandall PH, Scheibel AB. The hippocampal-dentate complex in temporal lobe epilepsy. Epilepsia. 1974;15:55–80.Shtrahman, M., Yeung, C., Nauen, D. W., Bi, G.-q. & Wu, X.-L. Probing vesicle dynamics in single hippocampal synapses.

Smedler, E., Malmersjo, S. & Uhlen, P. Network analysis of time-lapse microscopy recordings. doi:D - NLM: PMC4166320 OTO - NOTNLM.

Sloviter, R. S., Zappone, C. A., Harvey, B. D. & Frotscher, M. Kainic acid-induced recurrent mossy fiber innervation of dentate gyrus inhibitory interneurons: Possible anatomical substrate of granule cell hyperinhibition in chronically epileptic rats. The Journal of Comparative Neurology 494, 944-960, doi:10.1002/cne.20850 (2006).

Staley KJ, Otis TS, Mody I.. Membrane properties of dentate gyrus granule cells: comparison of sharp microelectrode and whole-cell recordings. J Neurophysiol. 1992 May;67(5):1346-58.

Sutula T, Cascino G, Cavazos J, Parada I, Ramirez L. Mossy fiber synaptic reorganization in the epileptic human temporal lobe. Ann Neurol. 1989 Sep;26(3):321–330.

Takechi H, Eilers J, Konnerth A. A new class of synaptic response involving calcium release in dendritic spines. Nature. 1998 Dec 24-31;396(6713):757-60.

Temprana, Silvio G., Mongiat, Lucas A., Yang, Sung M., Trinchero, Mariela F., Alvarez, Diego D., Kropff, E., Giacomini, D., Beltramone, N., Lanuza, Guillermo M. & Schinder, Alejandro F. Delayed Coupling to Feedback Inhibition during a Critical

Period for the Integration of Adult-Born Granule Cells. Neuron 85, 116-130, doi:http://dx.doi.org/10.1016/j.neuron.2014.11.023 (2015).

Toni, Nicolas, Diego A. Laplagne, et al. "Neurons Born in the Adult Dentate Gyrus Form Functional Synapses with Target Cells." *Nature Neuroscience* 11.8 (2008): 901–907. *NCBI PubMed*. Web.

Vale F.L., Pollock G, Benbadis S.R. Failed epilepsy surgery for mesial temporal lobe sclerosis: a review of the pathophysiology. Neurosurg Focus. 2012 Mar;32(3):E9. doi: 10.3171/2011.12.FOCUS11318.

Wieser HG, ILAE Commission on Neurosurgery of Epilepsy. Epilepsia. ILAE Commission Report. Mesial temporal lobe epilepsy with hippocampal sclerosis. 2004 Jun; 45(6):695-714.

Zhao, Chunmei, E. Matthew Teng, et al. "Distinct Morphological Stages of Dentate Granule Neuron Maturation in the Adult Mouse Hippocampus." *The Journal of Neuroscience* 26.1 (2006): 3–11. *www.jneurosci.org*. Web